molecular pharmaceutics

pubs.acs.org/molecularpharmaceutics

Article

Effect of Dopamine D_2 Receptor Antagonists on [^{18}F]-FEOBV Binding

Anna Schildt, Erik F.J. de Vries, Antoon T.M. Willemsen, Bruno Lima Giacobbo, Rodrigo Moraga-Amaro, Jürgen W.A. Sijbesma, Aren van Waarde, Vesna Sossi, Rudi A.J.O. Dierckx, and Janine Doorduin*

Cite This: *Mol. Pharmaceutics* 2020, 17, 865−872

Read Online

ACCESS | Metrics & More | Article Recommendations | Supporting Information

ABSTRACT: The interaction of dopaminergic and cholinergic neurotransmission in, e.g., Parkinson's disease has been well established. Here, D_2 receptor antagonists were used to assess changes in [^{18}F]-FEOBV binding to the vesicular acetylcholine transporter (VAChT) in rodents using positron emission tomography (PET). After pretreatment with either 10 mg/kg haloperidol, 1 mg/kg raclopride, or vehicle, 90 min dynamic PET scans were performed with arterial blood sampling. The net influx rate (K_i) was obtained from Patlak graphical analysis, using a metabolite-corrected plasma input function and dynamic PET data. [^{18}F]-FEOBV concentration in whole-blood or plasma and the metabolite-corrected plasma input function were not significantly changed by the pretreatments (adjusted $p > 0.07$, Cohen's d 0.28−1.89) while the area-under-the-curve (AUC) of the parent fraction of [^{18}F]-FEOBV was significantly higher after haloperidol treatment (adjusted $p = 0.022$, Cohen's $d = 2.51$) than in controls. Compared to controls, the AUC of [^{18}F]-FEOBV, normalized for injected dose and body weight, was nonsignificantly increased in the striatum after haloperidol (adjusted $p = 0.4$, Cohen's $d = 1.77$) and raclopride (adjusted $p = 0.052$, Cohen's $d = 1.49$) treatment, respectively. No changes in the AUC of [^{18}F]-FEOBV were found in the cerebellum (Cohen's d 0.63−0.74). Raclopride treatment nonsignificantly increased K_i in the striatum 1.3-fold compared to control rats (adjusted $p = 0.1$, Cohen's $d = 1.1$) while it reduced K_i in the cerebellum by 28% (adjusted $p = 0.0004$, Cohen's $d = 2.2$) compared to control rats. Pretreatment with haloperidol led to a nonsignificant reduction in K_i in the striatum (10%, adjusted $p = 1$, Cohen's $d = 0.44$) and a 40−50% lower K_i than controls in all other brain regions (adjusted $p < 0.0005$, Cohen's $d = 3.3$−4.7). The changes in K_i induced by the selective D_2 receptor antagonist raclopride can in part be quantified using [^{18}F]-FEOBV PET imaging. Haloperidol, a nonselective D_2/σ receptor antagonist, either paradoxically decreased cholinergic activity or blocked off-target [^{18}F]-FEOBV binding to σ receptors. Hence, further studies evaluating the binding of [^{18}F]-FEOBV to σ receptors using selective σ receptor ligands are necessary.

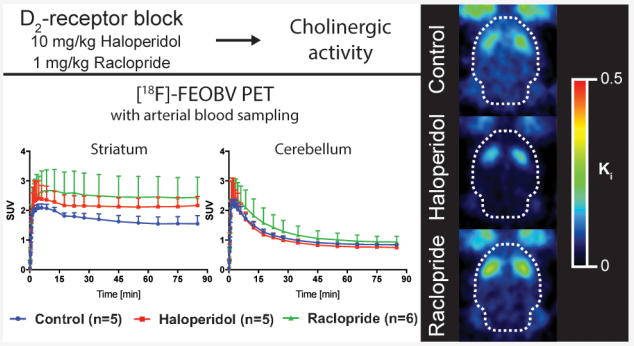

KEYWORDS: *animal studies, D_2 receptor, σ receptor, vesicular acetylcholine transporter, kinetic modeling, positron emission tomography, Parkinson's disease*

INTRODUCTION

Traditionally, Parkinson's disease is viewed as a neurodegenerative disorder that is characterized by motor impairments, including slowness of movement, muscle stiffness, and tremor. These motor symptoms result from the degeneration of dopaminergic neurons in the substantia nigra and the consequent deficiency of dopamine in brain regions that receive dopaminergic input from this brain region,[1] such as the striatum. It is now evident that Parkinson's disease also involves nonmotor symptoms that can be explained by the degeneration of multiple neurotransmitter systems,[2,3] including the cholinergic system. Loss of cholinergic neurons has been reported in Parkinson's disease and has been thought to play a significant role in cognitive decline and motor symptoms such as tremor.[4,5]

To gain more insight into the relation between dopaminergic and cholinergic neurotransmission in Parkinson's disease, the noninvasive imaging technique positron emission tomography (PET) can play an important role. [^{18}F]-FEOBV, a benzovesamicol analog, is a PET ligand that binds allosterically to the vesicular acetylcholine transporter (VAChT).[6−8] VAChT is expressed in presynaptic cholinergic neurons and transports acetylcholine into synaptic vesicles. While VAChT is not a direct marker of acetylcholine synthesis or release, it has

Received: October 31, 2019
Revised: February 3, 2020
Accepted: February 3, 2020
Published: February 3, 2020

been shown that the expression of VAChT can be used to study cholinergic neurons.[9,10] For example, clinical studies using [^{18}F]-FEOBV have revealed changes in the cholinergic system in patients with Parkinson's disease.[11,12]

Using microdialysis in rodents, it has been shown that the turnover of acetylcholine and its release into the synaptic cleft is increased after blocking of the dopamine D_2 receptors.[13−15] Additionally, an increased uptake or binding of benzovesamicol radioligands in the striatum has been reported after the block of D_2 receptors.[16−18] While the exact mechanisms leading to the increased binding of benzovesamicols following D_2 receptor block are unknown, it has been suggested that changes in the vesamicol binding site of the VAChT are dependent on cholinergic activity, e.g. increased acetylcholine release.[16] Here, we aimed to determine if acute blocking of the dopamine D_2 receptors would lead to increased accumulation of [^{18}F]-FEOBV as a measure of cholinergic activity. For this purpose, we chose the selective dopamine D_2/D_3 receptor antagonist raclopride and the less selective D_2 receptor antagonist haloperidol which have previously been used in this context and estimated cholinergic activity as measured by the net influx rate (K_i) estimated by Patlak graphical analysis.[16−19]

EXPERIMENTAL SECTION

Experimental Animals. The experiments were approved by the National Committee on Animal Experiments (CCD:AVD105002015166) and the Institutional Animal Care and Use Committee of the University of Groningen (IvD: 15166-01-003). Male Wistar rats (n = 18, Hsd/Cpb:WU, aged 12.2 ± 2.3 weeks, 364 ± 33 g) were obtained from Envigo (The Netherlands) and housed in groups in humidity and temperature-controlled (21 ± 2 °C) rooms with a 12 h/12 h light/dark cycle (lights on at 7 a.m.). Water and standard laboratory chow were supplied ad libitum. After arrival the rats were acclimatized for at least 7 days and then randomly divided in three groups treated with either vehicle (control, n = 6), 10 mg/kg haloperidol[19] (n = 6), or 1 mg/kg raclopride[20] (n = 6). The PET scans were executed between 1 and 5 p.m. No blinding of the investigators was possible during the experiment, but the data analysis was automated and, hence, independent of the operator.

PET Imaging. The rats were anesthetized with isoflurane (5% for induction, 1−2.5% for maintenance) in 95% oxygen, and eye salve was applied to prevent dehydration of the eyes. Rats were then injected intraperitoneally with 100 μL DMSO (control), 10 mg/kg haloperidol, or 1 mg/kg raclopride in 100 μL DMSO at 52 ± 10 min (range 44−80 min) before injection of [^{18}F]-FEOBV. One cannula was placed in the tail vein for injection of [^{18}F]-FEOBV, and a second was in the femoral artery for arterial blood sampling. A dedicated small animal PET scanner (Focus 220 MicroPET, Siemens Healthcare, USA) was used, and two rats were scanned simultaneously. For attenuation correction, a transmission scan with a ^{57}Co point source was performed before each emission scan. During the PET scan, the heart rate and oxygen saturation were monitored and heating pads were used to maintain the body temperature of the rats between 37 and 38 °C. [^{18}F]-FEOBV (28 ± 8 MBq, molar activity >300 000 GBq/mmol) was injected over 1 min at a rate of 1 mL/min via an infusion pump and a dynamic PET scan of 90 min was started simultaneously with injection. Synthesis of [^{18}F]-FEOBV was performed according to Mulholland et al. with adjustments to local infrastructure.[21]

An attenuation-weighted 2-dimensional ordered subset expectation-maximization algorithm (OSEM2D, 4 iterations, 16 subsets) following Fourier rebinning was used for iterative reconstruction of the list mode data binned into 24 frames (6 × 10, 4 × 30, 2 × 60, 1 × 120, 1 × 180, 4 × 300, 6 × 600 s). The data were normalized and corrected for scatter, attenuation, and decay. The resulting image matrix was 256 × 256 × 95 with a slice thickness of 0.796 mm and a pixel width of 0.633 mm.

One rat in the haloperidol treatment group died 54 min after the injection of [^{18}F]-FEOBV and was excluded from the analysis.

Arterial Blood Sampling and Metabolite Analysis. At approximately 10, 20, 30, 40, 50, 60, 90 s and 2, 3, 5, 7.5, 10, 15, 30, 60, and 90 min after [^{18}F]-FEOBV, injection blood samples (0.10−0.13 mL each) were drawn from the femoral artery. The same volume of heparinized saline was injected after collection of each blood sample to compensate for blood loss. Plasma was obtained by centrifugation of whole-blood for 5 min at 30 000g. An automated well-counter (Wizard2480, PerkinElmer, USA) was used to measure radioactivity (decay corrected) in 25 μL of whole-blood and 25 μL of plasma.

Metabolite analysis was performed for all plasma samples obtained between 1 and 90 min.[19] After acetonitrile (50 μL) was added to each sample, the samples were vortexed and centrifuged (3000g for 8 min). A 1 to 2 μL portion of the supernatant from each sample were pipetted onto a silica gel 60 F_{254} plate (Merck, Germany), and the elution was performed with a mixture of hexane/dichloromethane/diethyl ether/triethylamine (2.3/1/1/0.2). A phosphor storage screen (PerkinElmer, USA) was exposed overnight to the eluted silica plates and scanned the next day using a Cyclone (PerkinElmer, USA) phosphorescence imager. OptiQuant software 3 was used to obtain the percentage of intact tracer for correction of the plasma input curve.

PET Data Analysis. PET data analysis was performed using PMOD 3.9 software. Each individual PET image was automatically coregistered to a [^{18}F]-FEOBV template.[22] A volume of interest (VOI) atlas, containing frontal cortex, remainder of the cortex (referred to as "cortex"), striatum, thalamus, hypothalamus, hippocampus, brainstem, and cerebellum, was then placed on each coregistered PET image. For each individual rat, time−activity curves (kBq/mL) were generated for each VOI. Based on previous analysis from our laboratory, irreversible plasma input models were best suited for [^{18}F]-FEOBV quantification in rats. Irreversible plasma input models estimate the net influx rate ($K_i = K_1k_3/(k_2 + k_3)$) which estimates the irreversible binding but also the net influx of the radioligand. In this study, Patlak graphical analysis showed a lower variation of the net influx rate compared to the irreversible two-tissue compartment model (2TCM). K_i from Patlak graphical analysis was estimated with a stretch time of 10 min, whole-blood, and metabolite-corrected plasma input.[23]

Statistical Analysis. Statistical analysis was performed using SPSS 23. The area under the curve (AUC) was determined for the parent fraction, the plasma (with or without correction for metabolites) and whole-blood time-activity curves and the striatal and cerebellar time-activity curves. The time-activity curves for plasma, whole-blood, and brain regions were normalized to standardized uptake values (SUV = tissue activity concentration/(injected dose/body weight)). Differences in AUC between treatments were assessed using one-way analysis of variance (ANOVA).

https://dx.doi.org/10.1021/acs.molpharmaceut.9b01129
Mol. Pharmaceutics 2020, 17, 865−872

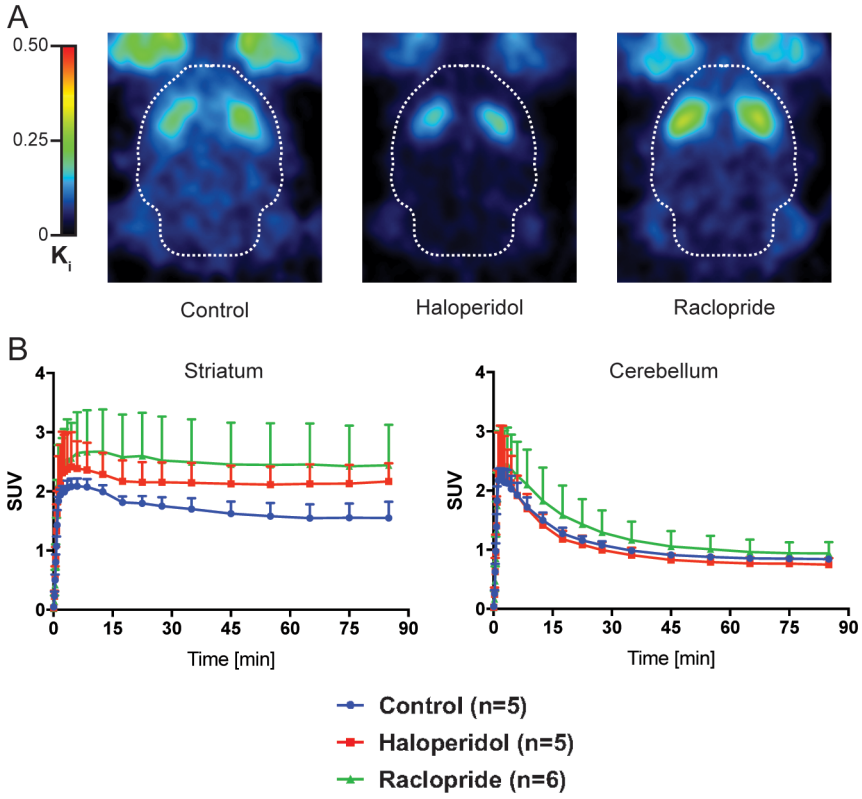

Figure 1. Uptake of [^{18}F]-FEOBV in the brain of control rats and rats pretreated with 10 mg/kg haloperidol or 1 mg/kg raclopride. The net influx rate (K_i) images of representative rats from each group are shown (A) as well as the time-activity curves of the striatum and cerebellum for all rats in each group (mean + SD) (B).

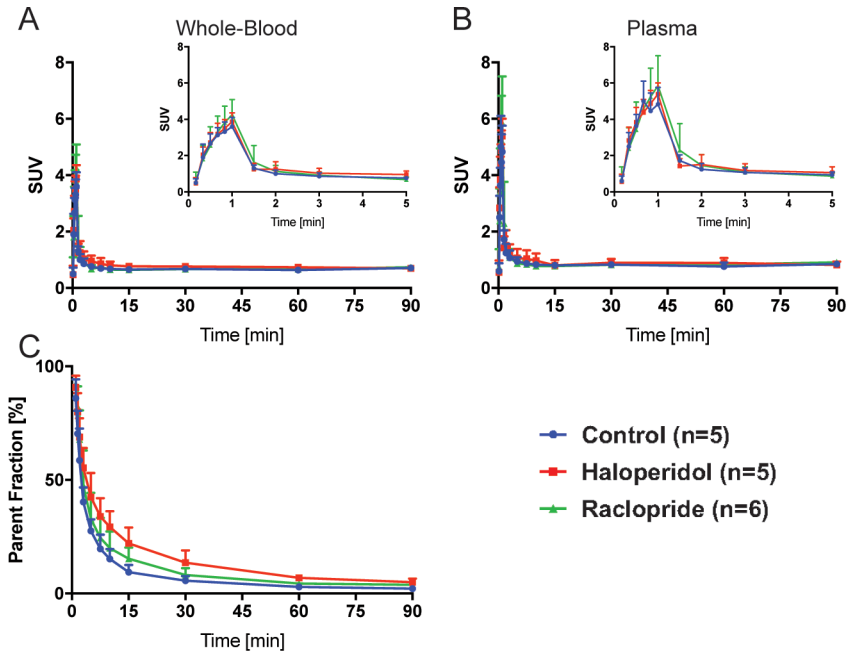

Figure 2. Time-activity curves of [^{18}F]-FEOBV uptake in whole-blood (A) and plasma (B) and the parent fraction of [^{18}F]-FEOBV (C) for control rats and rats pretreated with 10 mg/kg haloperidol or 1 mg/kg raclopride (mean + SD).

Posthoc analysis was performed using Bonferroni correction for multiple comparisons between control and treatments and the adjusted *p*-values are given.

For the K_i obtained from PET imaging, the differences between the three groups were assessed using generalized estimating equations (GEE) with treatment as a between-group factor, brain region as a within-subject factor, and treatment × brain region as the interaction. Posthoc tests for differences between treatments were performed for each brain region and corrected for multiple comparisons using the Bonferroni method. GEE was used to assess differences between the three groups while accounting for intraindividual

https://dx.doi.org/10.1021/acs.molpharmaceut.9b01129
Mol. Pharmaceutics 2020, 17, 865−872

Table 1. Net Influx Rate (K_i, [mL/cm^3·min], mean ± SD) of [^{18}F]-FEOBV in Brain Tissue in Control Rats and Rats Pretreated with 10 mg/kg Haloperidol or 1 mg/kg Raclopride and the Effect Size (Cohen's d) Comparing the Control Group to Each Pretreatment[a]

	control (n = 5)	haloperidol (n = 5)		raclopride (n = 6)	
brain region	K_i	K_i	Cohen's d	K_i	Cohen's d
brainstem	0.077 ± 0.013	0.044 ± 0.006	3.29	0.071 ± 0.011	0.52
cerebellum	0.062 ± 0.009	0.031 ± 0.002	4.66	0.045 ± 0.007	2.15
cortex	0.074 ± 0.010	0.044 ± 0.007	3.41	0.069 ± 0.010	0.49
frontal cortex	0.089 ± 0.012	0.050 ± 0.011	3.52	0.090 ± 0.022	0.06
hippocampus	0.074 ± 0.011	0.037 ± 0.008	3.95	0.062 ± 0.012	0.97
hypothalamus	0.090 ± 0.011	0.049 ± 0.007	4.40	0.082 ± 0.016	0.59
striatum	0.129 ± 0.032	0.117 ± 0.023	0.44	0.167 ± 0.038	1.09
thalamus	0.079 ± 0.012	0.044 ± 0.008	3.36	0.073 ± 0.013	0.49

[a] K_i (mL/cm^3·min), Cohen's d is between the control and treatment groups.

differences and repeated measures, i.e. the dependence of brain regions in each rat (within-subject). Cohen's d was calculated for each treatment group using the means and pooled standard deviation of the control and treatment group.[24]

Differences were deemed statistically significant with $p < 0.05$ (adjusted for multiple comparisons using Bonferroni correction if necessary). Effect sizes with Cohen's $d > 0.5$, 0.8, 1.2, and 2.0 were considered medium, large, very large, and huge, respectively.[25]

One rat of the control group showed an exceptionally large value for K_i as obtained by Patlak graphical analysis in all brain regions (>1.5× interquartile range) and was excluded from the analysis.

RESULTS

Tracer kinetics and Metabolism. The time-activity curves of [^{18}F]-FEOBV were analyzed for two brain regions representing the highest (striatum) and lowest (cerebellum) uptake of [^{18}F]-FEOBV. [^{18}F]-FEOBV showed an initial high uptake in both regions, with the highest [^{18}F]-FEOBV uptake in the striatum at approximately 3 to 4 min after injection in control and haloperidol treated rats and at 6 to 8 min in rats treated with raclopride (Figure 1). The area-under-the-curve (AUC) of the striatal time-activity curve tended to be higher in haloperidol (Cohen's d = 1.77) and raclopride treated rats (Cohen's d = 1.49) when compared to control rats, but these differences were not statistically significant ($F(2, 15) = 3.7$, p = 0.053). In the cerebellum, the highest initial uptake of [^{18}F]-FEOBV was found between 1 and 3 min, with a 9% and 14% higher uptake in haloperidol and raclopride treated rats, respectively, than in control rats. On average the AUC of the cerebellar time−activity curve tended to be increased in raclopride (Cohen's d = 0.74) and decreased in haloperidol treated rats (Cohen's d = 0.63), but this was not statistically significant ($F(2, 15) = 2$, p = 0.2).

The AUC of the plasma and whole-blood time-activity curve (Figure 2) was not significantly changed by pretreatment with haloperidol (plasma Cohen's d = 0.63, whole-blood Cohen's d = 1.10) or raclopride (plasma Cohen's d = 0.39, whole-blood Cohen's d = 0.41) compared to control rats (plasma, $F(2, 15) = 0.6$, p = 0.5; whole-blood, $F(2, 15) = 2.3$, p = 0.1). A statistically significant difference in the AUC of the parent fraction between the three groups was found ($F(2, 11) = 6$, p = 0.022). Posthoc tests revealed a statistically significantly higher AUC of the parent fraction in haloperidol treated rats when compared to controls (adjusted p = 0.022, Cohen's d = 2.51), while no statistically significant difference was found between the AUC of the parent fraction of the control and raclopride treatment groups (adjusted p = 0.6, Cohen's d = 1.16). Despite a statistically significant difference in the AUC of the parent fraction between the haloperidol and control rats, the difference in the AUC of the metabolite-corrected plasma curve was not significant ($F(2, 15) = 3.3$, p = 0.07; haloperidol, Cohen's d = 1.89; raclopride, Cohen's d = 0.28).

Net Influx Rate of [^{18}F]-FEOBV. Patlak graphical analysis revealed average K_i values ranging from 0.031 to 0.167 mL/cm^3·min for different treatment groups and brain regions. The highest K_i was found in the striatum, and the lowest in the cerebellum, for all three groups (Table 1). A statistically significant effect of treatment ($\chi^2(1, 2) = 40$, $p < 0.0001$) and brain region ($\chi^2(1, 7) = 691$, $p < 0.0001$) on the K_i of [^{18}F]-FEOBV was found, as well as a statistically significant interaction between treatment and brain region ($\chi^2(1, 13) = 3475$, $p < 0.0001$). Posthoc analysis revealed a statistically significant difference in K_i between control and haloperidol treated rats and between haloperidol and raclopride treated rats for all brain regions together (adjusted $p < 0.0001$), but no statistically significant difference was found between control and raclopride treated rats (adjusted p = 1). Comparison of the treatments in each individual brain region (Figure 3) revealed a statistically significant difference between haloperidol treated and control rats in brainstem, cerebellum, cortex, frontal cortex, hippocampus, hypothalamus, and thalamus (adjusted p

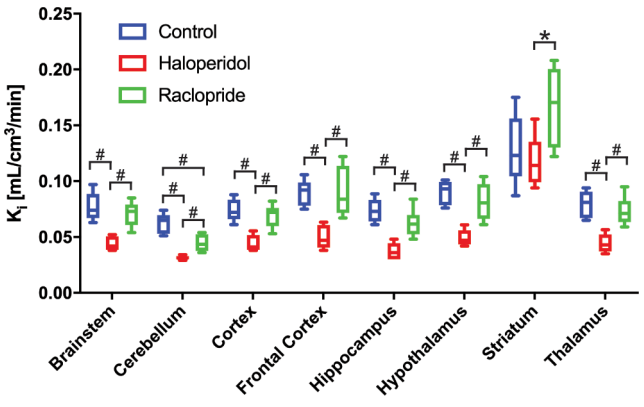

Figure 3. Net influx rate (K_i) of [^{18}F]-FEOBV in different brain regions for control rats and rats treated with 10 mg/kg haloperidol or 1 mg/kg raclopride (boxplot, box interquartile range, whiskers 1.5× interquartile range), and adjusted p-values from posthoc comparison of treatment × brain region interaction (* $p < 0.05$, # $p < 0.0005$).

https://dx.doi.org/10.1021/acs.molpharmaceut.9b01129
Mol. Pharmaceutics 2020, 17, 865−872

< 0.0005, Cohen's d 3.29−4.66), but not in striatum (adjusted p = 1, Cohen's d 0.44) most likely due to the large variation in K_i (coefficient of variation 23%) in this brain region. In all other brain regions, the K_i was statistically significantly decreased by an average of 45 ± 3%, with the largest decrease of 49−50% in the cerebellum and hippocampus and the lowest of 40% in the cortex. Contrarily, the only individual brain region with a significant difference between control and raclopride treated rats was the cerebellum (adjusted p = 0.0004, Cohen's d 2.15) with a decrease in K_i of 28%. In the striatum, an increase in K_i of 30% was found. Despite a large effect size, this difference did not reach the threshold for statistical significance (adjusted p = 0.1, Cohen's d 1.09). In the other brain regions, K_i was found to be decreased by 8 ± 5%, but this effect was not statistically significant (Cohen's d 0.06−0.97). Significant differences between haloperidol and raclopride treatment were found in all individual brain regions (adjusted p < 0.05) with an average difference in K_i of 60 ± 13% (42−81%).

DISCUSSION

In the current study, we have found changes in the net influx rate of [^{18}F]-FEOBV after acute treatment with D_2 receptor antagonists, using PET imaging. The specific D_2 receptor antagonist raclopride led to a statistically significant decrease in the net influx rate of [^{18}F]-FEOBV in the cerebellum and nonstatistically significant increase of the net influx rate in the striatum. In contrast, the less specific D_2 receptor antagonist haloperidol led to a decreased net influx rate in all brain regions except the striatum. Although haloperidol significantly decreased the metabolism of [^{18}F]-FEOBV, treatment with either raclopride or haloperidol did not affect the whole-blood, plasma, and the metabolite-corrected plasma input, showing that changes found in the net influx rate K_i were not due to hemodynamic differences.

Interestingly, we found a statistically significant decrease in the net influx rate of [^{18}F]-FEOBV in the cerebellum of rats treated with raclopride. Contrarily, a study by Efange et al. using the VAChT radioligand (+)-[^{125}I]-MIBT in rats found no change in the cerebellar uptake of (+)-[^{125}I]-MIBT after treatment with the D_2 receptor antagonist S-(−)-eticlopride.[26] In the same study, however, a significant increase in the uptake of the less specific (−)-[^{125}I]-MIBT in the cerebellum after spiperone (D_2 receptor antagonist) treatment was observed. The discrepancy between our and the study of Efange et al. could be related to the different D_2 receptor antagonists used and their varying binding affinities to the D_2 receptor and potential off-target binding.[27] Additionally, Efange et al. performed ex vivo biodistribution after 3 h, while we determined the net influx rate of [^{18}F]-FEOBV using Patlak graphical analysis using a 90 min PET acquisition. The difference in time, as well as the more specific quantification via PET imaging with pharmacokinetic modeling compared to the ex vivo distribution, could explain the differences between our study and the study of Efange et al. Previous studies showed only negligible binding of the D_2 receptor antagonist raclopride in the cerebellum of rats.[28,29] Additionally, it was also determined that raclopride binding in the striatum was saturated at 23.5 pmol/g[28] which could suggest that the higher dose of approximately 3 nmol/g (1 mg/kg) of raclopride used in our study could have led to increased off-target binding of raclopride to serotonergic or adrenergic receptors and thereby facilitated the decrease in the net influx rate of [^{18}F]-FEOBV via interaction with other neurotransmitters.[28]

While we found a decrease in [^{18}F]-FEOBV net influx rate in the cerebellum, the net influx rate and area-under-the-curve of [^{18}F]-FEOBV in the striatum tended to be increased after raclopride treatment as evidenced by the large effect size found between control and raclopride treated rats. Ingvar et al. showed increased uptake of the VAChT radioligand [^{18}F]-NEFA in the striatum of primates after raclopride or haloperidol treatment.[16] Similarly, Efange et al. showed increased striatal uptake of (+)-[^{125}I]-MIBT in rats pretreated with spiperone and S-(−)-eticlopride at 3 h after injection of (+)-[^{125}I]-MIBT.[17] In addition, after depletion of dopaminergic neurons in the rat striatum with 6-OHDA, a smaller spiperone-induced increase in (+)-[^{125}I]-MIBT uptake was found in the ipsilateral striatum, when compared to the contralateral side.[26] In a more recent study, Jin et al. showed a 1.5-fold increase in binding of the VAChT ligand [^{11}C]-TZ659 in striatum after treatment with S-(−)-eticlopride.[18] These findings indicate that D_2 receptor antagonism results in an increased binding of benzovesamicol radioligands in the striatum, most likely due to increased acetylcholine turnover facilitated by the antagonized D_2 receptor[13−15,30] and suggest that with lower variability of the net influx rate in the striatum a significant difference might have been found in our study. Hence, our study suggests that [^{18}F]-FEOBV could be capable of measuring increased cholinergic activity in rats after treatment with the D_2 receptor antagonist raclopride.

Raclopride tended to increase the net influx rate of [^{18}F]-FEOBV in the striatum, whereas, haloperidol, the other D_2 receptor antagonist used in this study, nonsignificantly decreased the net influx rate by 10%. In fact, haloperidol significantly reduced the net influx rate by up to 50% in all other brain regions. There are several possible explanations for this result. First, the overall reduction in the net influx rate after haloperidol pretreatment could suggest reduced cholinergic activity. Nevertheless, microdialysis experiments in rats treated with haloperidol indicate that the opposite is the case, as an increase in acetylcholine turnover was observed after haloperidol treatment.[15] Hence, it is unlikely that the results of our study can be explained by a decreased cholinergic activity due to haloperidol treatment.

Second, hemodynamic changes after haloperidol treatment could have reduced the uptake of [^{18}F]-FEOBV in the brain. Similar to a study by Mulholland et al., we used a high dose (10 mg/kg) of haloperidol. Mulholland found a reduction of [^{18}F]-FEOBV brain uptake and blood activity of up to 30 and 50%, respectively, when compared to control mice.[19] They suggested that hemodynamic changes after the high-dose haloperidol treatment were responsible for the reduced brain uptake.[19] We found the area-under-the-curve of the [^{18}F]-FEOBV parent fraction to be significantly higher compared to control rats, indicating a reduced metabolism of [^{18}F]-FEOBV after haloperidol pretreatment. However, no significant differences in the area-under-the-curve of the whole-blood or plasma activity curve of [^{18}F]-FEOBV (parent and metabolite), as well as no significant changes in the metabolite-corrected plasma input function (parent only) between the control and haloperidol group, were found although the determined effect sizes were large. Furthermore, we found no statistically significant differences in the influx rate constant K_1 obtained from the irreversible 2TCM between control and haloperidol or raclopride treated rats in any brain region (Supplemental

https://dx.doi.org/10.1021/acs.molpharmaceut.9b01129
Mol. Pharmaceutics 2020, 17, 865−872

Table 1). This suggests that hemodynamic changes did not change [^{18}F]-FEOBV delivery to the brain after haloperidol pretreatment in our study.

Third, it could be possible that due to the high dose of haloperidol used in this study not only D_2 receptors were occupied. Haloperidol binds to a variety of neuroreceptors, e.g. serotonergic, dopaminergic, or adrenergic receptors,[31] which could, in turn, have affected the net influx rate of [^{18}F]-FEOBV either directly by changes in cholinergic neurotransmission or indirectly via the dopaminergic or other neurotransmitter systems.

Another possible explanation for the reduced net influx rate of [^{18}F]-FEOBV could be the blocking of σ receptors by haloperidol pretreatment. Haloperidol has been described as a potent σ_1 receptor antagonist and σ_2 receptor agonist.[32] The binding affinity of vesamicol derivatives like [^{18}F]-FEOBV to σ receptors has been a topic of dispute. Some argued that most vesamicol-based radioligands, including [^{18}F]-FEOBV, should not be considered for VAChT imaging because of their binding affinity for σ receptors.[33,34] The binding affinity of (−)-FEOBV has been determined in vitro as 19.6 ± 1.1 and 209 ± 94 nM to rat VAChT and σ_1 receptors, respectively.[33,35] A study by Mulholland et al. investigated the effect of different σ ligands on brain uptake and blood activity of [^{18}F]-FEOBV in mice at three different time points after injection using ex-vivo biodistribution.[19] Donepezil and (+)-3-PPP did not influence [^{18}F]-FEOBV uptake in different brain regions or radioactivity levels in blood. However, donepezil is a σ_1 receptor agonist as well as an acetylcholine esterase inhibitor, whereas haloperidol is a σ_1 receptor antagonist. While haloperidol and (+)-3-PPP are both σ_1/σ_2 receptor ligands their binding affinities for each σ receptor are different suggesting different blocking of the σ receptors.[32] Indeed, haloperidol led to a 36% increase of [^{18}F]-FEOBV uptake in the striatum 240 min after injection, but to a reduction in whole brain uptake and blood activity at earlier time points in the study by Mulholland et al.[19] A biodistribution study by Efange et al. in young rats showed reduced [^{125}I]-MIBT uptake in the cerebellum (50%) and cortex (38%), in agreement with our study and increased [^{125}I]-MIBT uptake in the striatum after haloperidol treatment.[17] We did not find a statistically significant increase in the net influx rate of [^{18}F]-FEOBV in the striatum, nevertheless, as mentioned above the different time of assessment as well as quantification methods, i.e. PET imaging with pharmacokinetic modeling compared to ex vivo biodistribution, could explain these inconsistencies.

Further indication for binding of [^{18}F]-FEOBV to σ receptors could be the correlation of the σ receptor expression pattern with the reduced [^{18}F]-FEOBV net influx rate we found in our study after the haloperidol pretreatment. In the brain, σ receptors are found almost equally in most brain regions, with lower expression in the striatum and the highest expression in the brainstem.[36−38] This partly agrees with the decreased [^{18}F]-FEOBV net influx rate we found after haloperidol treatment. However, while the lowest decrease of the net influx rate was found in the striatum (10%), the largest reduction of approximately 50% was found in the cerebellum and hippocampus compared to the brainstem with 43%. This suggests that the decreased net influx rate partly follows the expression of σ receptors in the brain. Nevertheless, while the binding affinity of [^{18}F]-FOEBV to σ_1 receptors in rats has been determined as approximately 200 nM, it was recently shown that its binding affinity is approximately 10-fold lower in humans (2275 nM).[39] Thus, it is likely that the suggested binding of [^{18}F]-FEOBV to σ_1 receptors in rats, if any, will not affect imaging of VAChT in humans. When using haloperidol as a D_2 receptor antagonist its binding to other neuroreceptors should be considered, especially in studies using [^{18}F]-FEOBV. Additionally, it would be of interest to study the effect of a dopamine D_2 receptor agonist on [^{18}F]-FEOBV binding, in comparison to the effect of raclopride.

Lastly, it has been shown that isoflurane anesthesia decreases the release of acetylcholine in several brain regions, including striatum and cortex, in a dose-dependent manner.[40,41] Isoflurane is a widely used anesthetic in PET imaging studies in rodents which, at least for now, cannot be omitted during the procedure. As all rats in this study were treated with approximately the same dose of isoflurane a constant bias between the control and treatment groups can be assumed. Furthermore, the increase in [^{18}F]-FEOBV net influx rate in the striatum after treatment with raclopride suggests increased cholinergic activity after treatment, even if isoflurane inhibits the release of acetylcholine. This was also confirmed by biodistribution studies where mice were only anesthetized for short periods of time and using different anesthetics.[17,19] Hence, it is very unlikely that the reduced [^{18}F]-FEOBV net influx rate after haloperidol treatment was caused by isoflurane anesthesia. Furthermore, our study shows that acute changes in cholinergic activity can be evaluated using [^{18}F]-FEOBV even under isoflurane anesthesia.

CONCLUSION

In the present study, we showed that changes in cholinergic activity after treatment with the selective D_2 receptor antagonist raclopride and the nonselective D_2 receptor antagonist haloperidol can partly be quantified using [^{18}F]-FEOBV PET imaging. The seemingly decreased cholinergic activity after treatment with haloperidol appears to be due to off-target binding of [^{18}F]-FEOBV to σ receptors in rat brain. This hypothesis needs to be confirmed in further studies on the off-target binding of [^{18}F]-FEOBV to σ receptors in rat brain. Such off-target binding will probably not occur in the human brain due to interspecies differences in the binding affinities of [^{18}F]-FEOBV to σ receptors.

ASSOCIATED CONTENT

Supporting Information

The Supporting Information is available free of charge at https://pubs.acs.org/doi/10.1021/acs.molpharmaceut.9b01129.

Supplemental Table 1 Influx rate constant (K_1, [min^{-1}], mean ± SD) of [^{18}F]-FEOBV in brain tissue in control rats and rats pretreated with 10 mg/kg haloperidol or 1 mg/kg raclopride. K_1 was estimated using the 2-tissue compartmental model (PDF)

AUTHOR INFORMATION

Corresponding Author

Janine Doorduin − *Department of Nuclear Medicine and Molecular Imaging, University of Groningen, University Medical Center Groningen, Groningen 9700RB, The Netherlands*; Phone: +31-503610151; Email: j.doorduin@umcg.nl; Fax: +31-503611687

https://dx.doi.org/10.1021/acs.molpharmaceut.9b01129
Mol. Pharmaceutics 2020, 17, 865−872

Authors

Anna Schildt − *Department of Nuclear Medicine and Molecular Imaging, University of Groningen, University Medical Center Groningen, Groningen 9700RB, The Netherlands; Department of Physics and Astronomy, University of British Columbia, Vancouver, BC V6T 2B5, Canada;* orcid.org/0000-0001-7587-8318

Erik F.J. de Vries − *Department of Nuclear Medicine and Molecular Imaging, University of Groningen, University Medical Center Groningen, Groningen 9700RB, The Netherlands*

Antoon T.M. Willemsen − *Department of Nuclear Medicine and Molecular Imaging, University of Groningen, University Medical Center Groningen, Groningen 9700RB, The Netherlands*

Bruno Lima Giacobbo − *Department of Nuclear Medicine and Molecular Imaging, University of Groningen, University Medical Center Groningen, Groningen 9700RB, The Netherlands*

Rodrigo Moraga-Amaro − *Department of Nuclear Medicine and Molecular Imaging, University of Groningen, University Medical Center Groningen, Groningen 9700RB, The Netherlands*

Jürgen W.A. Sijbesma − *Department of Nuclear Medicine and Molecular Imaging, University of Groningen, University Medical Center Groningen, Groningen 9700RB, The Netherlands*

Aren van Waarde − *Department of Nuclear Medicine and Molecular Imaging, University of Groningen, University Medical Center Groningen, Groningen 9700RB, The Netherlands*

Vesna Sossi − *Department of Physics and Astronomy, University of British Columbia, Vancouver, BC V6T 2B5, Canada*

Rudi A.J.O. Dierckx − *Department of Nuclear Medicine and Molecular Imaging, University of Groningen, University Medical Center Groningen, Groningen 9700RB, The Netherlands*

Complete contact information is available at: https://pubs.acs.org/10.1021/acs.molpharmaceut.9b01129

Notes

The authors declare no competing financial interest.

■ ACKNOWLEDGMENTS

We thank David Vállez Garcia and Lara García Varela for advice on kinetic model selection and Paula Kopschina Feltes and Rolf Zijlma for their help with the setup of the metabolite analysis. The Djavad Mowafaghian Centre for Brain Health supported A.S. financially during this study.

■ REFERENCES

(1) Langston, J. W. The Parkinson's Complex: Parkinsonism Is Just the Tip of the Iceberg. *Ann. Neurol.* **2006**, *59* (4), 591−596.

(2) Braak, H.; Tredici, K. D.; Rüb, U.; de Vos, R. A. I.; Jansen Steur, E. N. H.; Braak, E. Staging of Brain Pathology Related to Sporadic Parkinson's Disease. *Neurobiol. Aging* **2003**, *24* (2), 197−211.

(3) Schapira, A. H. V.; Chaudhuri, K. R.; Jenner, P. Non-Motor Features of Parkinson Disease. *Nat. Rev. Neurosci.* **2017**, *18* (7), 435−450.

(4) Müller, M. L. T. M.; Bohnen, N. I. Cholinergic Dysfunction in Parkinson's Disease. *Curr. Neurol. Neurosci. Rep.* **2013**, *13* (9), 377.

(5) Kalia, L. V.; Lang, A. E. Parkinson's Disease. *Lancet* **2015**, *386*, 896−912.

(6) Ojeda, A. M.; Kolmakova, N. G.; Parsons, S. M. Acetylcholine Binding Site in the Vesicular Acetylcholine Transporter. *Biochemistry* **2004**, *43* (35), 11163−11174.

(7) Khare, P.; Mulakaluri, A.; Parsons, S. M. Search for the Acetylcholine and Vesamicol Binding Sites in Vesicular Acetylcholine Transporter: The Region around the Lumenal End of the Transport Channel. *J. Neurochem.* **2010**, *115* (4), 984−993.

(8) Bahr, B. A.; Parsons, S. M. Acetylcholine Transport and Drug Inhibition Kinetics in Torpedo Synaptic Vesicles. *J. Neurochem.* **1986**, *46* (4), 1214−1218.

(9) Arvidsson, U.; Riedl, M.; Elde, R.; Meister, B. Vesicular Acetylcholine Transporter (VAChT) Protein: A Novel and Unique Marker for Cholinergic Neurons in the Central and Peripheral Nervous Systems. *J. Comp. Neurol.* **1997**, *378* (4), 454−467.

(10) Ichikawa, T.; Ajiki, K.; Matsuura, J.; Misawa, H. Localization of Two Cholinergic Markers, Choline Acetyltransferase and Vesicular Acetylcholine Transporter in the Central Nervous System of the Rat: In Situ Hybridization Histochemistry and Immunohistochemistry. *J. Chem. Neuroanat.* **1997**, *13* (1), 23−39.

(11) Bohnen, N. I.; Kanel, P.; Zhou, Z.; Koeppe, R. A.; Frey, K. A.; Dauer, W. T.; Albin, R. L.; Müller, M. L. T. M. Cholinergic System Changes of Falls and Freezing of Gait in Parkinson's Disease. *Ann. Neurol.* **2019**, *85* (4), 538−549.

(12) Bedard, M.-A.; Aghourian, M.; Legault-Denis, C.; Postuma, R. B.; Soucy, J.-P.; Gagnon, J.-F.; Pelletier, A.; Montplaisir, J. Brain Cholinergic Alterations in Idiopathic REM Sleep Behaviour Disorder: A PET Imaging Study with 18F-FEOBV. *Sleep Med.* **2019**, *58*, 35−41.

(13) Ikarashi, Y.; Takahashi, A.; Ishimaru, H.; Arai, T.; Maruyama, Y. Regulation of Dopamine D1 and D2 Receptors on Striatal Acetylcholine Release in Rats. *Brain Res. Bull.* **1997**, *43* (1), 107−115.

(14) DeBoer, P.; Heeringa, M. J.; Abercrombie, E. D. Spontaneous Release of Acetylcholine in Striatum Is Preferentially Regulated by Inhibitory Dopamine D2 Receptors. *Eur. J. Pharmacol.* **1996**, *317* (2−3), 257−262.

(15) DeBoer, P.; Abercrombie, E. D. Physiological Release of Striatal Acetylcholine in Vivo: Modulation by D1 and D2 Dopamine Receptor Subtypes. *J. Pharmacol. Exp. Ther.* **1996**, *277* (2), 775−783.

(16) Ingvar, M.; Stone-Elander, S.; Rogers, G. A.; Johansson, B.; Eriksson, L.; Parsons, S. M.; Widén, L. Striatal D2/Acetylcholine Interactions: PET Studies of the Vesamicol Receptor. *NeuroReport* **1993**, *4* (12), 1311−1314.

(17) Efange, S. M. N.; Langason, R. B.; Khare, A. B. Age-Related Diminution of Dopamine Antagonist Stimulated Vesamicol Receptor Binding. *J. Nucl. Med.* **1996**, *37* (7), 1192−1197.

(18) Jin, H.; Zhang, X.; Yue, X.; Liu, H.; Li, J.; Yang, H.; Flores, H.; Su, Y.; Parsons, S. M.; Perlmutter, J. S. Kinetics Modeling and Occupancy Studies of a Novel C-11 PET Tracer for VAChT in Nonhuman Primates. *Nucl. Med. Biol.* **2016**, *43* (2), 131−139.

(19) Mulholland, G. K.; Wieland, D. M.; Kilbourn, M. R.; Frey, K. A.; Sherman, P. S.; Carey, J. E.; Kuhl, D. E. [18F]Fluoroethoxy-Benzovesamicol, a PET Radiotracer for the Vesicular Acetylcholine Transporter and Cholinergic Synapses. *Synapse* **1998**, *30* (3), 263−274.

(20) Alexoff, D. L.; Vaska, P.; Marsteller, D.; Gerasimov, T.; Li, J.; Logan, J.; Fowler, J. S.; Taintor, N. B.; Thanos, P. K.; Volkow, N. D. Reproducibility of 11C-Raclopride Binding in the Rat Brain Measured with the MicroPET R4: Effects of Scatter Correction and Tracer Specific Activity. *J. Nucl. Med.* **2003**, *44* (5), 815−822.

(21) Mulholland, G. K.; Jung, Y.-W.; Wieland, D. M.; Kilbourn, M. R.; Kuhl, D. E.; et al. Synthesis of [18F]Fluoroethoxy-Benzovesamicol, a Radiotracer for Cholinergic Neurons. *J. Labelled Compd. Radiopharm.* **1993**, *33* (7), 583−591.

(22) Vállez Garcia, D.; Casteels, C.; Schwarz, A. J.; Dierckx, R. A. J. O.; Koole, M.; Doorduin, J. A Standardized Method for the Construction of Tracer Specific PET and SPECT Rat Brain Templates: Validation and Implementation of a Toolbox. *PLoS One* **2015**, *10* (3), No. e0122363.

(23) Patlak, C. S.; Blasberg, R. G.; Fenstermacher, J. D. Graphical Evaluation of Blood-to-Brain Transfer Constants from Multiple-Time Uptake Data. *J. Cereb. Blood Flow Metab.* **1983**, *3* (1), 1−7.

(24) Berben, L.; Sereika, S. M.; Engberg, S. Effect Size Estimation: Methods and Examples. *Int. J. Nurs. Stud.* **2012**, *49* (8), 1039−1047.

(25) Sawilowsky, S. S. New Effect Size Rules of Thumb. *J. Mod. Appl. Stat. Methods* **2009**, *8* (2), 597−599.

(26) Efange, S. M. N.; Langason, R. B.; Khare, A. B.; Low, W. C. The Vesamicol Receptor Ligand (+)-Meta-[125I]-Iodobenzyltrozamicol {(+)-[125I]-MIBT} Reveals Blunting of the Striatal Cholinergic Response to Dopamine D2 Receptor Blockade in the 6-Hydroxydopamine (6-OHDA)-Lesioned Rat: Possible Implications for Parkinson'. *Life Sci.* **1996**, *58* (16), 1367−1374.
(27) Martelle, J. L.; Nader, M. A. A Review of the Discovery, Pharmacological Characterization, and Behavioral Effects of the Dopamine D2-like Receptor Antagonist Eticlopride. *CNS Neurosci. Ther.* **2008**, *14* (3), 248−262.
(28) Köhler, C.; Hall, H.; Ögren, S.-O.; Gawell, L. Specific in Vitro and in Vivo Binding of 3H-Raclopride a Potent Substituted Benzamide Drug with High Affinity for Dopamine D-2 Receptors in the Rat Brain. *Biochem. Pharmacol.* **1985**, *34* (13), 2251−2259.
(29) Hume, S. P.; Myers, R.; Bloomfield, P. M.; Opacka-Juffry, J.; Cremer, J. E.; Ahier, R. G.; Luthra, S. K.; Brooks, D. J.; Lammertsma, A. A. Quantitation of Carbon-11-Labeled Raclopride in Rat Striatum Using Positron Emission Tomography. *Synapse* **1992**, *12* (1), 47−54.
(30) Racagni, G.; Cheney, D. L.; Trabucchi, M.; Costa, E. In Vivo Actions of Clozapine and Haloperidol on the Turnover Rate of Acetylcholine in Rat Striatum. *J. Pharmacol. Exp. Ther.* **1976**, *196* (2), 323−332.
(31) Tyler, M. W.; Zaldivar-Diez, J.; Haggarty, S. J. Classics in Chemical Neuroscience: Haloperidol. *ACS Chem. Neurosci.* **2017**, *8* (3), 444−453.
(32) Rousseaux, C. G.; Greene, S. F. Sigma Receptors [σ Rs]: Biology in Normal and Diseased States. *J. Recept. Signal Transduction Res.* **2016**, *36* (4), 327−388.
(33) Barthel, C.; Sorger, D.; Deuther-Conrad, W.; Scheunemann, M.; Schweiger, S.; Jäckel, P.; Roghani, A.; Steinbach, J.; Schüürmann, G.; Sabri, O.; et al. New Systematically Modified Vesamicol Analogs and Their Affinity and Selectivity for the Vesicular Acetylcholine Transporter - A Critical Examination of the Lead Structure. *Eur. J. Med. Chem.* **2015**, *100*, 50−67.
(34) Ogawa, K.; Shiba, K. In Vivo and in Vitro Characteristics of Radiolabeled Vesamicol Analogs as the Vesicular Acetylcholine Transporter Imaging Agents. *Contrast Media Mol. Imaging* **2018**, *2018*, 1−14.
(35) Kovac, M.; Mavel, S.; Deuther-Conrad, W.; Méheux, N.; Glöckner, J.; Wenzel, B.; Anderluh, M.; Brust, P.; Guilloteau, D.; Emond, P. 3D QSAR Study, Synthesis, and in Vitro Evaluation of (+)-5-FBVM as Potential PET Radioligand for the Vesicular Acetylcholine Transporter (VAChT). *Bioorg. Med. Chem.* **2010**, *18* (21), 7659−7667.
(36) McCann, D. J.; Weissman, A. D.; Su, T.-P. Sigma-1 and Sigma-2 Sites in Rat Brain: Comparison of Regional, Ontogenetic, and Subcellular Patterns. *Synapse* **1994**, *17* (3), 182−189.
(37) Bouchard, P.; Quirion, R. [3H]1,3-Di(2-Tolyl)Guanidine and [3H](+)Pentazocine Binding Sites in the Rat Brain: Autoradiographic Visualization of the Putative Sigma1 and Sigma2 Receptor Subtypes. *Neuroscience* **1997**, *76* (2), 467−477.
(38) Ramakrishnan, N. K.; Visser, A. K. D.; Rybczynska, A. A.; Nyakas, C. J.; Luiten, P. G. M.; Kwizera, C.; Sijbesma, J. W. A.; Elsinga, P. H.; Ishiwata, K.; Dierckx, R. A. J. O.; et al. Sigma-1 Agonist Binding in the Aging Rat Brain: A MicroPET Study with [11C]SA4503. *Mol. Imaging Biol.* **2016**, *18* (4), 588−597.
(39) Helbert, H.; Wenzel, B.; Deuther-Conrad, W.; Luurtsema, G.; Szymanski, W.; Brust, P.; Feringa, B.; Dierckx, R. A. J. O.; Elsinga, P. H. Pd Catalyzed Cross-coupling of [^{11}C]MeLi and Its Application in the Synthesis and Evaluation of a Potential PET Tracer for the Vesicular Acetylcholine Transporter (VAChT). *J. Labelled Compd. Radiopharm.* **2019**, *62* (S1), S238.
(40) Westphalen, R. I.; Desai, K. M.; Hemmings, H. C. Presynaptic Inhibition of the Release of Multiple Major Central Nervous System Neurotransmitter Types by the Inhaled Anaesthetic Isoflurane. *Br. J. Anaesth.* **2013**, *110* (4), 592−599.
(41) Shichino, T.; Murakawa, M.; Adachi, T.; Nakao, S.; Shinomura, T.; Kurata, J.; Mori, K. Effects of Isoflurane on in Vivo Release of Acetylcholine in the Rat Cerebral Cortex and Striatum. *Acta Anaesthesiol. Scand.* **1997**, *41* (10), 1335−1340.

https://dx.doi.org/10.1021/acs.molpharmaceut.9b01129
Mol. Pharmaceutics 2020, 17, 865−872